Electronic Supporting Information

Chiral Recognition for the Complexation Dynamics of β-Cyclodextrin with the Enantiomers of 2-Naphthyl-1-ethanol

Hao Tang,[a] Andria S.M. Sutherland,[a] Lana M. Osusky,[a] Yan Li,[b] Josef F. Holzwarth[b] and Cornelia Bohne*[a]
[a]Department of Chemistry, University of Victoria, PO Box 3065, Victoria, BC V8W 3V6, Canada.
[b] Fritz-Haber-Institut, Department of Physical Chemistry Faradayweg 4-6, 14195 Berlin, Germany.

Index

Determination of the equilibrium constant K_{11} for the 1:1 NpOH/β-CD complex. 2
Equations S1-S11 2

NpOH triplet decay in the presence of β-CD and nitrite quenching studies 3
Figures S1 and S2 3
Figure S3 4

Time-resolved emission spectra (TRES) and determination of the NpOH monomer and excimer emission intensities 4
Figure S4 4
Equations S12-S15 4/5

Analysis of the binding isotherms for the formation of 2:2 NpOH:β-CD complexes 5
Equations S16-S29 5/6

Dependence of the C_{EE} values with the K_E values 6
Figure S5 6

Stopped-flow kinetics for the formation of the EE complex 7
Figure S6 7

Simulation of stopped-flow experiments 7
Figure S7 8

Global analysis of the kinetics for EE formation 9
Figure S8 9

Derivation of the relationship between the overall kinetics for 2:2 complex and *EE* complex formation 10
Equations S30-S39 10/11
Table S1 11

Determination of the equilibrium constant K_{11} for the 1:1 NpOH/β-CD complex.

Binding isotherms were determined at a low NpOH concentration of 5 μM where the 2:2 complex was not present in any significant amount. The fluorescence spectra were integrated between 300 nm and 375 nm. The binding isotherm was fit numerically using the Scientist 3 software (Micromath). The total concentration of β-CD ($[H_0]$) is defined as the independent variable. The equilibrium concentration of free host ([H]), free guest ([G]), 1:1 complex ([HG]) and the fluorescence emission intensity (I_{mon}) are defined as dependent variables. The emission efficiency for the 1:1 complex (C_{11}) and the equilibrium binding constant for the 1:1 complex (K_{11}) are defined as parameters in the model. R, the ratio between the fluorescence emission intensity ($I_{mon,0}$) of NpOH in the absence of β-CD and the total concentration of NpOH ($[G_0]$, 5 μM), is a constant for each independent experiment. R normalizes the emission efficiency for free NpOH for each experiment and therefore C_{11} is a relative emission intensity that is constant for different experiments. This normalization is required because different settings on the fluorimeter lead to different absolute fluorescence intensity values for different experiments.

$$[HG] = K_{11}[G][H] \quad \text{(S1)}$$

$$[H] = [H_0] - [HG] \quad \text{(S2)}$$

$$[G] = 5 \times 10^{-6} - [HG] \quad \text{(S3)}$$

$$I_{Mon} = R \times ([G] + C_{11}[HG]) \quad \text{(S4)}$$

$$\text{where } R = \frac{I_{mon,0}}{G_0} \quad \text{(S5)}$$

The ranges for the dependent variables were:

$$0 < [H] < 0.01 \text{ M} \quad \text{(S6)}$$

$$0 < [G] < 5\ \mu\text{M} \quad \text{(S7)}$$

$$0 < [HG] < 5\ \mu\text{M} \quad \text{(S8)}$$

K_{11} was related to both the formation of E and N. The binding isotherm for the 1:1 complex only leads to the determination of K_{11} because there is no spectroscopic signature that can be used to distinguish between N and E. The emission efficiencies for N and E are very similar because the lifetimes for both complexes are the same. Therefore, the same emission efficiency (C_{11}) was assumed for both 1:1 complexes. As a consequence, K_{11} corresponds to the sum of K_E and K_N.

$$I_{Mon} = C_{Np}[Np] + C_{11}[N] + C_{11}[E] \quad \text{(S9)}$$

$$I_{Mon} = C_{Np}[Np] + C_{11}(K_N + K_E)[Np][CD] \quad \text{(S10)}$$

$$I_{Mon} = C_{Np}[Np] + C_{11}K_{11}[Np][CD] \quad \text{(S11)}$$

NpOH triplet decay in the presence of β-CD and nitrite quenching studies.

The decay for the triplet excited state of NpOH in water followed a mono-exponential decay, whereas in the presence of β-CD a fast and a slow decay were observed. The time scales over which these decays occur were quite different (Fig. S1 and S2). In the presence of nitrite anions as a quencher this difference was enhanced because nitrite anions quench the triplet NpOH with short lifetime more efficiently than the long-lived triplet. A step-wise approach was employed to the fit the data. Decays were collected simultaneously at long (Fig. S1) and short (Fig. S2) collection times. The values for the observed rate constants depend critically on the off-set value a_0 at the end of the decay. This value was determined from the decay over a long collection time and was fixed for all fits. The decay in the long collection time was fit to a mono-exponential decay to recover a value for k_{obs2} (Fig. S1). The fit was started at a time that was ten times longer than the estimated short lifetime, since at this start time the contribution from the short-lived component was negligible. The decay at short collection times includes the decay for the short- and long-lived triplets and requires the fit of the data to the sum of two exponentials (eq. 4 in the paper). However, the long-lived decay is not well defined over this short time scale. For this reason, the values of a_0 and k_{obs2} were fixed for the fit. The observed rate constant recovered with this stepwise procedure are similar to those obtained by fitting the whole decays to a sum of two exponentials. However, the k_{obs} values are more precise and smaller errors were recovered. The values for a_1 and a_2 were recovered from the fit collected over a short time window.

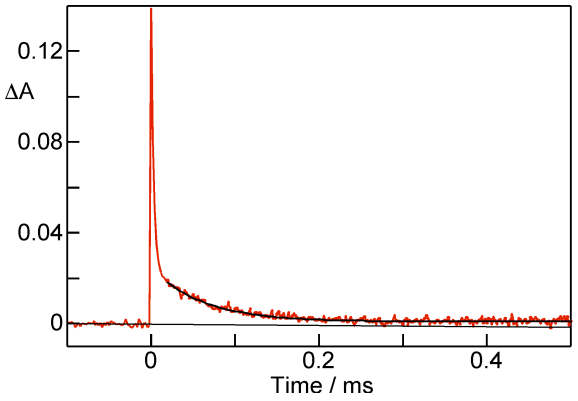

Figure S1. Triplet excited state decay (red) for (*S*)-NpOH (150 μM) in the presence of β-CD (10 mM) and $NaNO_2$ (0.35 mM). The data were fit to a mono-exponential decay after the decay of the fast component (black) with a fixed a_0 value determined from the data points at the end of the decay.

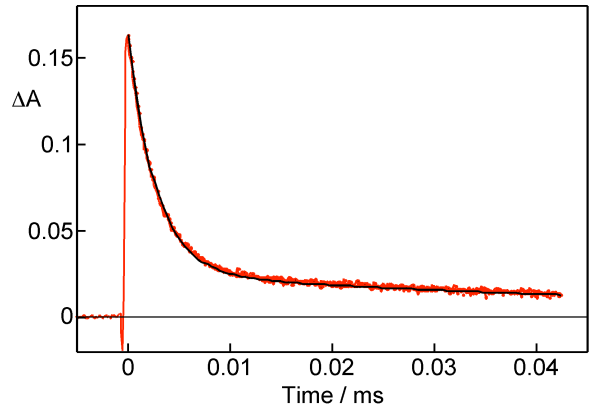

Figure S2. Triplet excited state decay (red) for (*S*)-NpOH (150 μM) in the presence of β-CD (10 mM) and $NaNO_2$ (0.35 mM). The data were fit to equation 4 in the paper (black) where values of a_0 and k_{obs2} were fixed and the values for k_{obs1}, a_1 and a_2 were recovered.

The quenching plots for the short- and long-lived triplet states by nitrite anions were linear (Fig. S3) and the quenching rate constants were obtained using equation 5 in the paper.

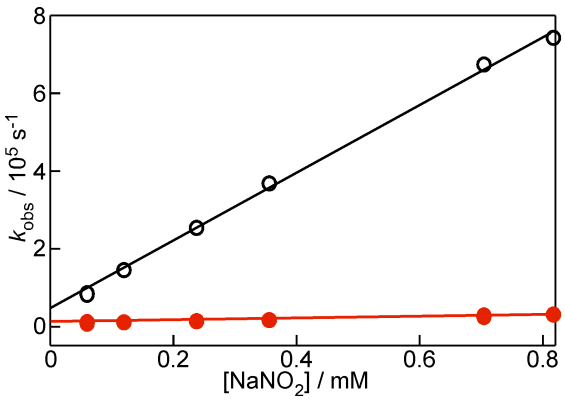

Figure S3. Quenching plots for the short- (black, open symbols) and long-lived (red, closed symbols) triplet states of (S)- NpOH (150 μM) by nitrite anions in the presence of 10 mM β-CD.

Time-resolved emission spectra (TRES) and determination of the NpOH monomer and excimer emission intensities.

The TRES at short delays contained the short-lived emission from the monomers of NpOH and the excimer emission from the *EE* complex. As the delays were lengthened the TRES evolved to the broad excimer emission from *EE*.

The determination of the binding isotherm for *EE* requires the correction of the emission intensity for the contribution of monomer emission from *E*, *N*, *EN* and *NN*.

The emission intensity where the monomer predominantly emits (I_{330}) was integrated between 322 nm and 338 nm, while the emission intensity where the excimer predominantly emits (I_{390}) was integrated between 382 nm and 398 nm. The monomer (I_{Mon}) and excimer intensities (I_{Ex}) need to be corrected for the intensities of the other species (eqs. S12 and S13), where f_1 is the fraction of the monomer intensity at 330 nm that contributes to the emission intensity at 390 nm and f_2 is the fraction of the excimer emission intensity at 390 nm that contributes to the emission intensity at 330 nm.

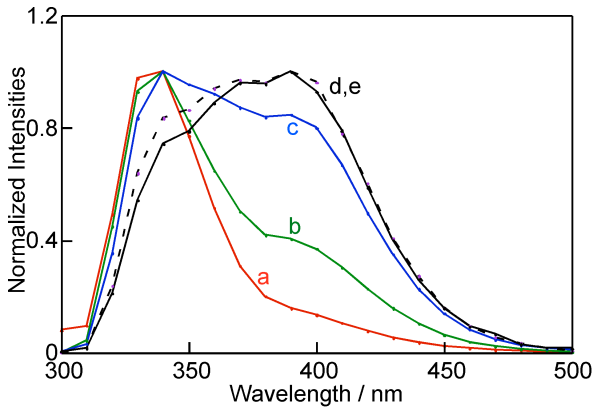

Figure S4. Normalized TRES for (R)-NpOH (150 μM) in the presence of β-CD (10 mM) with the following delays: a, red: 0-50 ns; b, green: 100-150 ns; c, blue:200-250 ns; d, dashed black: 300-350ns and e, black: 400-450 ns.

$$I_{390} = I_{Mon} f_1 + I_{Ex} \qquad \text{(S12)}$$

$$I_{330} = I_{Mon} + I_{Ex} f_2 \quad \text{(S13)}$$

The value for f_1 was determined to be 0.036 ± 0.002 from the NpOH emission spectrum in water. The excimer emission of NpOH was only observed in the presence of β-CD, and its spectrum was determined using TRES. The value of f_2 was determined to be 0.565 ± 0.007. Substituting the values for f_1 and f_2 into equations S12 and S13, and rearranging the equations led to:

$$I_{Mon} = 1.02 I_{330} - 0.58 I_{390} \quad \text{(S14)}$$

$$I_{Ex} = 1.02 I_{390} - 0.037 I_{330} \quad \text{(S15)}$$

The corrected monomer emission (I_{Mon}) for NpOH in the absence of β-CD was normalized with respect to the NpOH concentration in order to compare experiments performed on different days.

Analysis of the binding isotherms for the formation of 2:2 NpOH:β-CD complexes.
The excimer emission corresponds to the formation of the *EE* complex. The binding isotherm was fit using the Scientist 3 software. The equilibria for the formation of the 1:1 complexes (*E* and *N*) and for all three 2:2 complex (*EE*, *NN*, *EN*) are coupled and the binding isotherm for *EE* contains information for all equilibria (see scheme 2 in the paper). The total concentration of β-CD ($[H_0]$) is defined as the independent variable. The emission efficiency C_{EE} corresponds to the relative emission efficiency that was normalized to the monomer emission for NpOH in the absence of β-CD ($[G]_0$) and is constant for different experiments. The equilibrium concentrations for *H*, *G*, *E*, *N*, *EE*, *EN*, *NN* and the fluorescence emission intensity for *EE* (I_{EE}) were defined as dependent variables. The relative emission efficiency for the *EE* complex (C_{EE}), the equilibrium constant for the *E* complex (K_E) and the equilibrium constant for the *EE* complex (K_{EE}) were defined as parameters in the model. The total concentration of NpOH species was 150 μM.

$$[E] = K_E [G][H] \quad \text{(S16)}$$

$$[N] = (K_{11} - K_E)[G][H] \quad \text{(S17)}$$

$$[EE] = K_{EE} [E]^2 \quad \text{(S18)}$$

$$[EN] = K_{EN} [E][N] \quad \text{(S19)}$$

$$[NN] = K_{NN} [N]^2 \quad \text{(S20)}$$

$$[H_0] = [H] + [E] + [N] + 2([EE] + [EN] + [NN]) \quad \text{(S21)}$$

$$1.50 \times 10^{-4} = [G] + [E] + [N] + 2([EE] + [EN] + [NN]) \quad \text{(S22)}$$

$$I_{Ex} = C_{EE} [EE] \quad \text{(S23)}$$

The ranges for the dependent variables were:

$$0 < [\mathrm{H}] < 0.01\ \mathrm{M} \quad \text{(S24)}$$

$$0 < [\mathrm{E}] < 150\ \mu\mathrm{M} \quad \text{(S25)}$$

$$0 < [\mathrm{N}] < 150\ \mu\mathrm{M} \quad \text{(S26)}$$

$$0 < [\mathrm{EE}] < 75\ \mu\mathrm{M} \quad \text{(S27)}$$

$$0 < [\mathrm{EN}] < 75\ \mu\mathrm{M} \quad \text{(S28)}$$

$$0 < [\mathrm{NN}] < 75\ \mu\mathrm{M} \quad \text{(S29)}$$

The values for K_{EE}, K_{NN} and K_{EN} were considered equal based on the observation of one relaxation process in the kinetics for *EE* formation and the values for K_E were fixed to incremental values between 0 and 1,100 M^{-1}, where the latter value corresponds to K_{11}.

Dependence of the C_{EE} values with the K_E values.

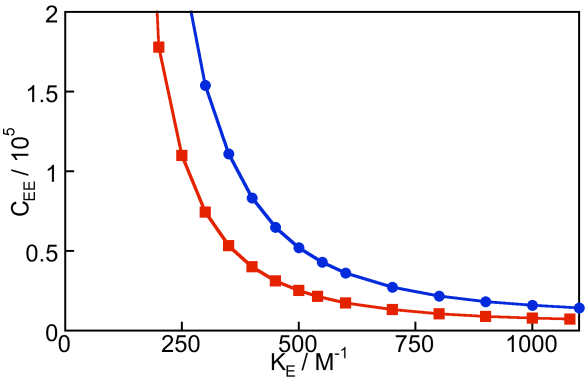

Figure S5. Dependence of C_{EE} recovered from the fit of the binding isotherm for different K_E values (red squares: (S)-NpOH; blue circles: (R)-NpOH)

Stopped-flow kinetics for the formation of the *EE* complex.

All kinetic traces fit adequately to an exponential function when fit individually. Figure S6 shows the fits for the trace with the largest amplitude (300 μM (R)-NpOH, 100 μM β-CD) and the trace with the smallest amplitude (50 μM (R)-NpOH, 50 μM β-CD). The residuals were random in all cases.

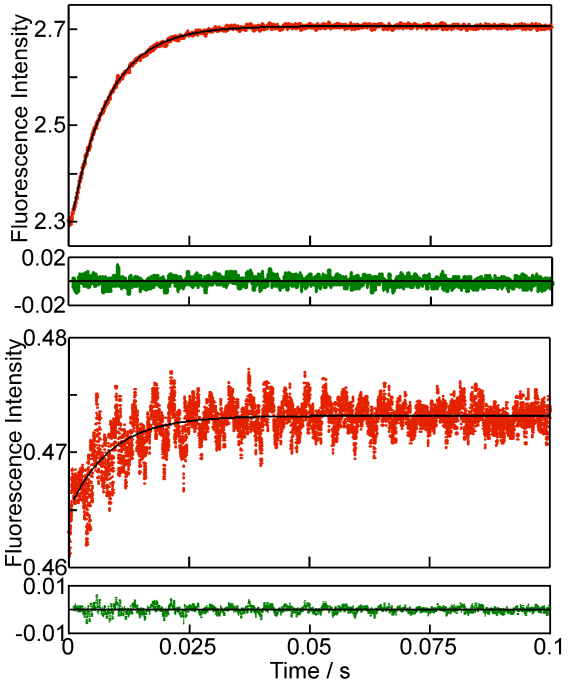

Figure S6. Kinetics for the formation of *EE* (red) fit to a monoexponential function (black). Top: 300 μM (R)-NpOH, 100 μM β-CD and bottom: 50 μM (R)-NpOH, 50 μM β-CD. The residuals are shown in green under each kinetic trace.

Simulation of stopped-flow experiments.

Simulations of the kinetics were conducted to check to what extent a difference between the rate constants for the formation of different 2:2 complexes (*EE*, *EN* and *NN*) would lead to two relaxation processes that can be differentiated in the kinetic measurements. The model for the simulations included the formation of the *E* and *N* 1:1 complexes as fast equilibria (K_E and K_N), and the formation of the 2:2 complexes were expressed by their respective association (k_+^{EE}, k_+^{EN} and k_+^{NN}) and dissociation rate constants (k_-^{EE}, k_-^{EN} and k_-^{NN}). The simulations were performed with the Pro-Kineticist II software and random noise was added by selecting a signal-to-noise ratio in the software that was similar to that observed in the experiments. The simulated data were then fit to the same model used to fit the experimental data (Scheme 3 in the paper) and the residuals between the simulated data and the fit were analyzed. Non-random residuals indicated that the parameters used in the simulations would be apparent in the kinetic experiment as an additional relaxation process.

The simulated kinetic traces were generated by two methods: (i) Varying the association rate constants for the *NN* (k_+^{NN}) and *EN* complexes (k_+^{EN}) while other parameters (K_E, K_N, k_+^{EE} and the

dissociation rate constants for all 2:2 complexes) were fixed. The dissociation rate constants for all 2:2 complexes were set to the same value. (ii) Varying the dissociation rate constants for the *NN* (k_{-}^{NN}) and *EN* complex (k_{-}^{EN}) while other parameters (K_E, K_N, k_{-}^{EE} and the association rate constants for all 2:2 complexes) were fixed. The association rate constants for all 2:2 complexes were set to the same value. Moreover, for methods (i) and (ii) the simulations were conducted under three different conditions to check how the ratio of K_E to K_N affected the differentiation of two kinetic relaxation processes: (a) the value of K_E was equal to that of K_N. (b) The value of K_E was higher than that of K_N, e.g. the value of K_E was 5 times higher than that of K_N. (c) The value of K_E was lower than that of K_N, e.g. the value of K_E was 5 times lower than that of K_N. An example for a simulation is shown in figure S7 when K_E is equal to K_N. Deviations were observed when the difference in the association rate constants for *EE* compared to *EN* and *NN* was larger than 5%. Residuals in panels "b", "c" and "d" in figure S7 were considered acceptable while residuals in panels "a" and "e" were considered to have significant deviations. Deviations were observed at different relative values depending on the scenarios (a) to (c) described above. The maximum differential before deviations between the simulated data and the model were observed were 25% between k_{+}^{EE} and k_{+}^{EN}/k_{+}^{NN} and 20% for the dissociation rate constants.

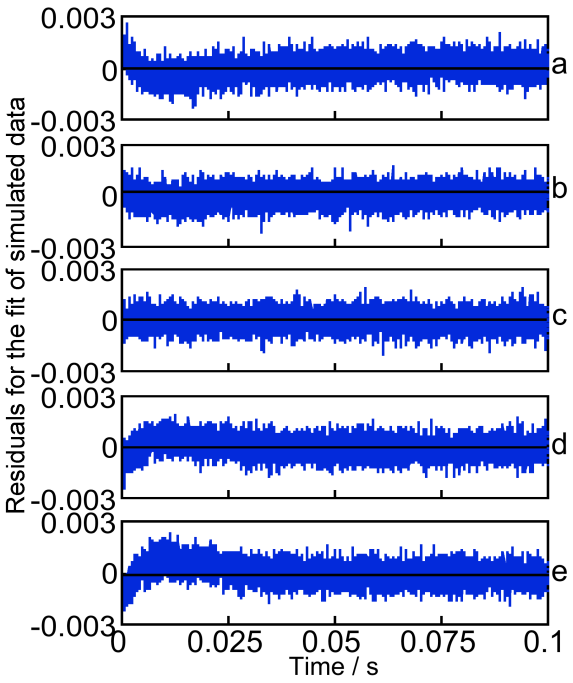

Figure S7. Residuals between simulated data and the model used for analysis of the experimental data. The simulated data were generated with the following values: [NpOH] = 300 μM, [β-CD] = 100 μM, K_E = 500 M^{-1}, K_N = 500 M^{-1}, k_{+}^{EE} = 9.28 × 10^5 M^{-1} s^{-1}, the dissociation rate constants for all 2:2 complexes were set to 115 s^{-1}. The association rate constants for *EN* and *NN* had the same value and were set to different percentages of k_{+}^{EE}: (a) 90%, (b) 95%, (c) 100%, (d) 105%, (e) 110%.

Global analysis of the kinetics for *EE* formation.

The kinetics at the different concentrations of NpOH and β-CD were simultaneously fit to the mechanism shown in scheme 3 using a global analysis method in Pro-Kineticist II (Applied Photophysics). The residuals for all kinetic traces were random (Fig. S8).

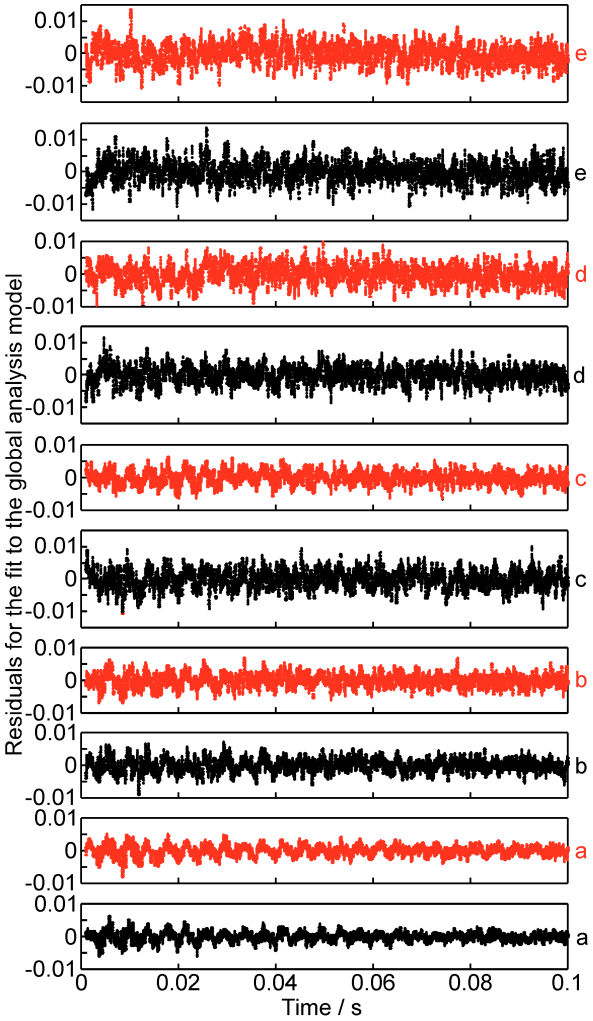

Figure S8. Residuals between the experimental data and the fit using global analysis for the mechanism shown in scheme 3 in the paper. (R)-NpOH was mixed with β-CD (black: 50 μM; red: 100 μM) at various concentration of (R)-NpOH: a, 50 μM; b, 100 μM; c, 150 μM; d, 200 μM and e, 300 μM.

Derivation of the relationship between the overall kinetics for 2:2 complex and *EE* complex formation.

The overall formation of 2:2 complexes leads to the following differential equation:

$$\frac{d[Np_2 \bullet CD_2]}{dt} = k_+^{22}[Np \bullet CD]^2 - k_-^{22}[Np_2 \bullet CD_2] \qquad (S30)$$

while the differential equation for the formation of the *EE* complex is given by:

$$\frac{d[EE]}{dt} = k_+^{EE}[E]^2 - k_-^{22}[EE] \qquad (S31)$$

The concentration of the 2:2 complexes is related to the concentration of the individual complexes. The assumption was made that the equilibrium constants for *EE*, *EN* and *NN* are the same.

$$[Np_2 \bullet CD_2] = K_{EE}[E]^2 + K_{EN}[E][N] + K_{NN}[N]^2 \qquad (S32)$$

$$[Np_2 \bullet CD_2] = K_{EE}\left([E]^2 + [E][N] + [N]^2\right) \qquad (S33)$$

$$[N] = \frac{K_N}{K_E}[E] \qquad (S34)$$

$$[Np_2 \bullet CD_2] = \left(1 + \frac{K_N}{K_E} + \left(\frac{K_N}{K_E}\right)^2\right) K_{EE}[E]^2 \qquad (S35)$$

$$[E]^2 = \frac{[EE]}{K_{EE}} \qquad (S36)$$

$$[Np \bullet CD] = [E] + [N] = \left(1 + \frac{K_N}{K_E}\right)[E] \qquad (S37)$$

Substituting equations S35 and S37 into equation S30 and substituting $[E]^2$ by equation S36:

$$\frac{d\left(1 + \frac{K_N}{K_E} + \left(\frac{K_N}{K_E}\right)^2\right)[EE]}{dt} = k_+^{22}\left(1 + \frac{K_N}{K_E}\right)^2[E]^2 - k_-^{22}\left(1 + \frac{K_N}{K_E} + \left(\frac{K_N}{K_E}\right)^2\right)[EE] \qquad (S38)$$

$$\frac{d[EE]}{dt} = \frac{\left(1 + \frac{K_N}{K_E}\right)^2}{\left(1 + \frac{K_N}{K_E} + \left(\frac{K_N}{K_E}\right)^2\right)} k_+^{22} [E]^2 - k_-^{22} [EE] \qquad (S39)$$

Table S1. Limiting values for the association (k_+^{EE}) and dissociation (k_-^{EE}) rate constants and equilibrium constants for *EE* formation derived from the fitting of kinetic data ($K_{EE,sf}$) and of fluorescence data ($K_{EE,flu}$), and the relative emission efficiency (C_{EE}).

	NpOH	k_+^{EE} **/ 10^5 M^{-1} s^{-1}**	k_-^{EE} **/ 10^2 s^{-1}**	$K_{EE,sf}$ **/ 10^3 M^{-1}**	$K_{EE,flu}$ **/ 10^3 M^{-1}**	C_{EE} **/ 10^4**
$K_E = K_{11}$	(R)-	9.2 ± 0.4	1.11 ± 0.05	8.3 ± 0.5	7.8 ± 0.3	4.30 ± 0.08
	(S)-	9.6 ± 0.5	1.63 ± 0.02	5.9 ± 0.3	6.0 ± 0.3	2.16 ± 0.04
$K_E = K_{11}$	(R)-	6.9 ± 0.3	1.11 ± 0.05	6.2 ± 0.4	5.8 ± 0.2	1.43 ± 0.03
($K_N = 0$)	(S)-	7.2 ± 0.4	1.63 ± 0.02	4.4 ± 0.2	4.5 ± 0.2	0.71 ±0.01
$K_N = K_{11}$	(R)-	not defined	1.11 ± 0.05	not defined	5.8 ± 0.2	∞
($K_E = 0$)	(S)-	not defined	1.63 ± 0.02	not defined	4.5 ± 0.2	∞